RSC Publishing Faraday Discussions

Probing the selectivity of Li+ and Na+ cations on noradrenaline at the molecular level

Journal:	*Faraday Discussions*
Manuscript ID	FD-ART-11-2018-000186.R1
Article Type:	Paper
Date Submitted by the Author:	01-Dec-2018
Complete List of Authors:	Ishiuchi, Shun-ichi; Tokyo Institute of Technology, Chemical Resources Laboratory Wako, Hiromichi; Tokyo Institute of Technology, Chemical Resources Laboratory Xantheas, Sotiris; Pacific Northwest National Laboratory, Physical Sciences Division Fujii, Masaaki; Tokyo Institute of Technology, Chemical Resources Laboratory

Probing the selectivity of Li^+ and Na^+ cations on noradrenaline at the molecular level

Shun-ichi Ishiuchi,[1] Hiromichi Wako,[1] Sotiris S. Xantheas[*2,3] and Masaaki Fujii[*1]

[1] Laboratory for Chemistry and Life Science, Institute of Innovative Research, Tokyo Institute of Technology, 4259, Nagatsuta-cho, Midori-ku, Yokohama, 226-8503, Japan

[2] Advanced Computing, Mathematics and Data Division, Pacific Northwest National Laboratory, 902 Battelle Boulevard, P.O. Box 999, MS K1-83, Richland, WA 99352, United States

[3] Department of Chemistry, University of Washington, Seattle, WA 98195, United States

Abstract

Although several mechanisms concerning the biological function of lithium salt, a drug having tranquilizing abilities, have been proposed so far, the key mechanism for its selectivity and subsequent interaction with neurotransmitters has not been established yet. We report ultraviolet (UV) and infrared (IR) spectra under ultra-cold conditions of Li^+ and Na^+ complexes of noradrenaline (NAd, norepinephrine), a neurotransmitter responsible for the body's response to stress or danger, in an effort to provide a molecular level understanding of the conformational changes of NAd due to its interactions with these two cations. A detailed analysis of the IR spectra, aided by quantum chemical calculations, reveals that the Li^+-noradrenaline (NAd-Li^+) complex forms only an extended structure, while the NAd-Na^+ and protonated (NAd-H^+) complexes form both folded and extended structures. This conformational preference of the NAd-Li^+ complex is further explained from considering specific conformational distributions in solution. Our results clearly discern the unique structural motifs that Li^+ adopts when interacting with NAd compared with other abundant cations in the human body (Na^+) and can form the basis towards a molecular level understanding of the selectivity of Li^+ in biological systems.

---

* Corresponding authors: MF: mfujii@res.titech.ac.jp, SSX: sotiris.xantheas@pnnl.gov

I. Introduction

The tranquilizing abilities of lithium salt have been known since the 19th century,[1] when it was introduced as medication by Cade in 1949.[2] Nowadays, the most common form of a lithium-based tranquilizer is lithium carbonate. Several mechanisms concerning the biological function of lithium salt have been proposed such as that Li^+ interferes with some processes involving monoamine neurotransmitters, like noradrenaline, dopamine and serotonin, by enhancing secretion, inhibiting the re-uptaking and the metabolic process or producing some signaling molecules in several enzymes.[3-6] However, the key mechanisms of its biological function have not been fully established yet. One plausible and simple scenario is that the direct interactions between Li^+ and the monoamine neurotransmitters interferes with the the aforementioned processes.[7] This idea is quite intriguing for chemists, because they have the experimental and theoretical tools necessary to probe the structures and the underlying interactions in ionic clusters at the molecular level and further investigate the origins of the selectivity of various ions interacting with biologically important molecules.

In this work we focus on the interaction between NorAdrenaline (or norepinephrine, NAd) and cations such as Li^+ and Na^+. NAd and adrenaline (epinephrine) are catecholamine neurotransmitters released from the inner layer of the adrenal glands in response to sudden external stress stimuli, which they counter by transmitting more energy to the muscles via the raising of the blood sugar and arterial pressure. Furthermore, NAd's role in causing depression and Attention Deficit Hyperactivity Disorder (ADHD) has been discussed.[8-10] Because of the interest in understanding NAd's molecular recognition by receptors, several of its stable conformations have been previously investigated both theoretically and experimentally. Nagy *et al*. reported that there are three types of stable conformations on the amine chain of protonated noradrenaline (NAd-H^+).[11] They are denoted as T-, G1- and G2-type, corresponding to the *Trans*- (T) and *Gauche*-configurations (G) around the C1-C2 dihedral angle (see Figure 1). Their relative stability was reported both in the gas and solution phases. According to their calculation, the T conformer is the most stable in the solution phase, while the G1 conformer is more stable in the gas phase. In our previous work, we have reported conformer-selected infrared (IR) and ultraviolet (UV) spectra of NAd-H^+ measured

under ultra-cold isolated conditions by using the electrospray cold ion trap technique.[12] As a result, five conformers were identified and three of them were assigned to the G1-type conformer having different orientations of the catechol OHs and the two others to the T-type conformer. The observation of the T conformer which is ~10 kJ mol^{-1} less stable than the G1 conformer was attributed to the kinetic trapping effect, i.e. the T conformer, which is the most stable in solution, still retains its conformation in the gas phase during the electrospray process.

The present study extends our previous work by considering the interaction of NAd with the Li^+ and Na^+ cations and offers a critical comparison of their conformations with the ones reported for NAd-H^+. Although several efforts to investigate the conformations of both NAd[13-16] and NAd-H^+[11-12, 17-18] have been reported in the past, alkali metal ion complexes of NAd have not been reported yet. The strong interaction between alkali metal cations and NAd should significantly affect its conformation and may result in structural patterns that have an ion dependency.

Experimental techniques such as UV-UV hole burning[19] and IR dip spectroscopies[20] are appropriate for assigning the structures[21-29] and conformers[30-43] of ionic and neutral clusters[44-45]. In addition, when these techniques are aided by first principles quantum mechanical calculations of the energetics, structures and IR spectra of the various conformers, they are able to sort through the large number of conformational isomers which exist for these extended systems.[46-55] We therefore applied electrospray cold ion trap techniques[21, 24, 30, 56-57] to NAd-M^+ (M = Li and Na) and measured the conformer-selected UV and IR spectra. These measurements were complemented with electronic structure calculations. The comparison of the current results with those of NAd-H^+, reveal that NAd-Li^+ revealed a specific conformer-distribution. Such a specific distribution of conformations could affect the binding efficiency by the receptor and may be the key mechanism explaining the biological function of Li^+. The paper is organized as follows: in section 2 we outline the experimental and computational details. In section 3 we present the stable conformations and the UVPD and UV-UV HB spectra of the NAd-Li^+ and NAd-Na^+ complexes as well as their assignments. Final conclusions and a comparison with the NAd-H^+ structures are outlined in section 4.

II. Experimental and Computational Details

The details of the experimental setup were described elsewhere.[30] Noradrenaline (purchased from Aldrich) and MCl (M = Li, Na) were dissolved to pure degassed methanol (0.3 and 0.2 mM, respectively). The solution was electrosprayed and fine droplets were drawn into vacuum through a glass capillary which was heated to 60°C. The entrance of the glass capillary was metalized and a high voltage (-4.5 kV) was applied. Ions were desolvated through the glass capillary, introduced to a higher vacuum region via a skimmer and guided to a Quadrupole Mass Spectrometer (Q-MS: Extrel) by a hexapole ion guide. The mass of each species was selected by the Q-MS and introduced to a cryogenic 3-dimensional Quadrupole Ion Trap (QIT) made of copper via a quadrupole ion deflector and a octopole ion guide. The QIT was mounted on the second stage of a double stage closed cycle He refrigerator (Sumitomo: RDK-408D2) and was cooled down to 4 K. There, He gas at room temperature was introduced and cooled down by the copper electrodes of the QIT. The trapped ions were cooled down to ~10 K by the cold He buffer gas.[30] Afterwards, a tunable UV laser (probe laser) was introduced and the generated photo fragments were ejected into a Time Of Flight Mass Spectrometer (TOF-MS) and detected. The TOF-MS signal (tenfold-amplified by a preamplifier) was recorded by a fast digitizer board (NI: PXIe-5160). By monitoring the photo fragment intensity and scanning the wavelength of the UV laser, the UV photo dissociation (UVPD) spectra were recorded.

To obtain the conformer-selected UV spectra, UV-UV hole burning (HB) spectroscopy was employed. In this method, another tunable UV laser (burn laser) was introduced to the cryogenic QIT at 1 ms before the probe laser. Between the irradiation of the burn and probe lasers, a tickle RF pulse[12, 30, 58] was applied to the entrance end-cup of the QIT to eject photo fragments produced by the burn laser. By monitoring the photo fragment signal due to the probe laser, whose wavelength was fixed to a certain band observed in the UVPD spectrum, the wavelength of the burn laser was scanned. Since the signal intensity due to the probe laser is proportional to the population of a certain conformer at zero-

vibrational level of electronic ground state, if the wavelength of the burn laser is resonant to any electronic transitions of that conformer and excites it to electronically excited levels, a decrease of the ion signal is observed, reflecting the depopulation of the zero-vibrational level of the certain conformer. Such signal depletion is observed only when the electronic transitions occur in the certain conformer monitored by the probe laser; thus, conformer-selected UV spectra (UV-UV HB spectra) can be measured.

Instead of the burn UV laser, a tunable IR OPO laser (Surelite EX / LaserVision) was employed to measure conformer-selected IR spectra. Similarly to the UV-UV HB spectroscopy, by scanning the frequency of the IR laser with a simultaneous monitoring of the photo fragment signal due to the UV laser, conformer-selected IR spectra can be measured. We hereafter refer to this method as IR dip spectroscopy. The probe laser was operated at 20 Hz, while the burn laser and the IR laser at 10 Hz. Therefore, the probe-laser-only and double resonance signals were obtained alternatively. By dividing the latter by the former, the long term fluctuations of the source condition can be offset.[59]

To exhaustively search for all possible structures related to the conformation of the amine chain, the 2-D potential energy surface along the two dihedral angles around the C1-C2 and C2-C3 atoms was calculated. Figure 1 shows the definition of these angles and the pivot C1-C3 atoms of the conformational isomers of NAd-H^+ that were used as starting points to investigate the isomers of NAd-Li^+ and NAd-Na^+ following the procedure: the T-STR1 conformer of NAd-H^+ was chosen as the initial structure and H^+ was replaced by either Li^+ or Na^+. At every 10˚ intervals for each dihedral angle, the other internal coordinates were optimized at the CAM-B3LYP/aug-cc-pVDZ level of theory using Gaussian09[60]. The calculated 2-D plots of the potential energy surface of each complex are shown in Figure 2. In total, six local minima (labeled A, A', B, B', C and C') were found. The A/A', B/B' and C/C' pairs have the same conformation on the amine chain while the orientation of the catechol OHs are different (corresponding to STR1 and STR3). Therefore, three stable conformations exist on the amine chain. They were labeled T, G1 and G2, respectively, based on the conformations of NAd-H^+ (cf. Figure 1).

Assuming the combination of the three conformations of the amine chain and the four

orientations of catechol OHs as initial structures, full geometry optimizations at the RI-CC2/aug-cc-pVDZ level, which was also used for NAd-H^+ in our previous work,[12] was carried out by using TURBOMOLE (version 7.0.1)[61] and 12 stable structures were obtained for each complex.

III. Results and discussion

a. Stable conformations of the NAd-Li^+ and NAd-Na^+ complexes

The 12 stable structures obtained using the procedure outlined in the previous section for the NAd-Li^+ and NAd-Na^+ complexes are shown in Figures 3 and 4. Their relative stabilization energies including zero-point energy corrections (ZPC) are collected in Table 1. In all structures the lone pair of the amino group coordinates to the metal cation. In addition, the T conformers have an electrostatic interaction between M^+ (M = Li and Na) and the oxygen atom of the amine chain, whereas the G1 and G3 conformers have an electrostatic interaction between M^+ and the benzene ring. The stabilization energies are different depending on the orientation of catechol OHs, however, the relative energies of each conformation of the amine chain roughly follow the trend T < G1 < G2 in the NAd-Li^+ complex and G1 < T < G2 in the NAd-Na^+ complex, the latter order being the same for the NAd-H^+ complex.[12] It is therefore clear that the NAd-Li^+ complex already has a different conformational distribution than the NAd-H^+ and NAd-Na^+ ones.

b. UVPD and UV-UV HB spectra of the NAd-Li^+ and NAd-Na^+ complexes

Figure 5 shows the UVPD spectra of NAd-Li^+ and NAd-Na^+ complexes together with the ones of NAd-H^+ for comparison. For the NAd-Li^+ complex, photo dissociation signals were observed at m/z = 115 and 158 corresponding to $CH_2(OH)$-CH_2-NH_2 and H_2O loss, respectively, while only the former dissociation channel was observed for the NAd-Na^+ complex, resulting in a single photo fragment at m/z = 131. The UVPD spectra of both complexes were measured by detecting this dissociation channel.

In the NAd-Li^+ complex (Figure 5a) the most intense band was observed at 34,962

cm^{-1}. The UV laser was scanned down to 33,800 cm^{-1}, however no other band was observed. This spectral feature is totally different from that of NAd-H^+ (Figure 5c), in which a long progression was observed starting from 33,827 cm^{-1}. These electronic transitions were assigned to the G1 structure and the ~1,000 cm^{-1} redshift compared to other conformers was attributed to the contribution of a $\pi\sigma^*$ state to S_1 state.[12] Therefore, the lack of the red-shifted progression for the NAd-Li^+ complex implies that a conformer similar to G1 does not exist for that complex. On the other hand, the red-shifted progression seen before for the NAd-H^+ complex does appear in the NAd-Na^+ complex (Figure 5b). In addition, the spectral pattern around 35,000 cm^{-1} is close to that of NAd-H^+. These results suggest that the conformational distribution in the NAd-Na^+ complex is similar to that of NAd-H^+.

To further distinguish between conformers, the UV-UV HB spectra were measured. Figure 6a shows the UV-UV HB spectra of the NAd-Li^+ complex (6A-D), together with the UVPD spectrum for comparison (6b). By carefully probing the observed bands in the UVPD spectrum, four different UV-UV HB spectra were recorded. Since every band observed in the UVPD spectrum was also observed in any of the four HB spectra, it can be concluded that the NAd-Li^+ complex forms four different conformers under ultra-cold conditions. The most red-shifted bands observed in each HB spectrum are assigned to the 0-0 transition of each conformer. Their frequencies are collected in Table 2. By comparing the four HB spectra, it was found that conformers A (Li) and B (Li) give similar spectral patterns, which were also present in the conformers C (Li) and D (Li).

Figure 7a shows the UVPD and UV-UV HB spectra of the NAd-Na^+ complex. Four different conformers (A – D) were also identified for this complex. Their UVPD spectra are shown in Figure 7b. The most red-shifted bands observed in each HB spectra were assigned to the 0-0 transitions and their frequencies are listed in Table 2. Only conformer A (Na) shows a large red-shift (~1,000 cm^{-1}) among the other conformers, which implies that NAd-Na^+ does adopt the G1 conformer structure.

c. Structural assignments of the NAd-Li^+ complex

In order to assign the structures of each conformer, conformer-selected IR spectra

were measured using the IR dip spectroscopy. Figures 8a-d show the IR dip spectra of the NAd-Li^+ complex measured by probing the 0-0 transitions of each conformer. Even though they arise from different isomers, they give very similar IR spectra. This finding strongly suggests that the four conformers have the same structure on the amine chain, while adopting different orientations of the catechol OHs, i.e., they are OH rotamers. The most blue-shifted band observed at ~3,658 cm^{-1} and the strong band at ~3,594 cm^{-1} are assigned to the free and intra-molecular hydrogen-bonded OHs of catechol, respectively. Note that the corresponding ones for NAd-H^+ were observed at 3,660 ~ 3,665 and 3,592 ~ 3,600 cm^{-1}, respectively.[12] A sharp band observed between them is assigned to the free OH stretch of the amine chain based on the comparison with the spectra for NAd-H^+. The weak bands observed at ~3,375 and ~3,320 cm^{-1} are assigned to the antisymmetric and symmetric NH_2 stretches. The experimentally observed frequencies are presented in Table 3.

To assign the amine chain structure, the conformer-selected IR spectra of the NAd-Li^+ complex were compared with those of NAd-H^+. As mentioned in the Introduction, five different conformers were identified in the case of NAd-H^+, three of them being G1-type conformers and the other two T-type conformers. Figures 8e and 8f show the representative IR spectrum of each NAd-H^+ conformer which has been reported in our previous work.[12] Their spectra are clearly different in both the OH and NH stretching regions. In the OH stretching region, the T conformer shows three bands at 3,600, 3,651 and 3,664 cm^{-1}, respectively, with the middle one missing in the G1 conformer. These bands are assigned to the hydrogen-bonded OH of catechol, the free OH of the amine chain and the free OH of catechol, respectively. According to our calculations, the OH stretching bands of the second and third ones overlap in the G1 conformer. In the IR spectra of the NAd-Li^+ complex, three OH stretching bands are clearly observed, a finding suggesting that the conformation of the amine chain of all the conformers of the NAd-Li^+ complex is clearly of the T-type structure. In addition, the observed frequencies of the NH_2 stretches are also close to those of the T conformer of NAd-H^+, which also supports the above-mentioned assignment.

To further confirm this assignment, normal mode analyses were carried out for the 12 structures presented in Figure 3. The calculated frequencies, listed in Table 3, were linearly

scaled by 0.973 for the OH stretches and 0.951 for the others.[12] The calculated spectra, shown in Figure 8g, suggest that the frequencies of the intra-molecular H-bonded OH stretches of catechol are predicted at ~3,590 cm^{-1} for the T and G1 conformers, while those of G2 conformers are ~10 cm^{-1} lower. In addition, the free OH stretch of the amine chain appears red-shifted with respect to the free OH stretch of catechol in the T conformers, but blue-shifted in the G2 conformers. The calculated spectral shifts of the G2 conformers are in qualitative agreement with the experimental results. In the G1 conformers the free OH stretches of the amine chain and catechol are within 1~5 cm^{-1} of each other, while the difference between them is 7 ~ 19 cm^{-1} in the T conformers, compared 17 ~ 20 cm^{-1} in the experiment. Thus, the OH stretches of the T conformers are close to the observed ones. For the NH stretching region, the two NH stretching bands are predicted to have very weak intensities. The lower frequency band is assigned to the symmetric stretch of NH_2, while the higher one to the antisymmetric stretch. The frequencies of the symmetric stretch are predicted to be ~3,285 cm^{-1} in the T conformers and ~3,275 cm^{-1} for the G1 and G2 conformers. On the other hand, the antisymmetric stretch appears at ~3,365 cm^{-1} in the T and G1 conformers, and at ~3,355 cm^{-1} in the G2 conformers. Therefore, the NH stretches of the T conformers are close to the experimental results. The above results suggest that the observed four conformers of the NAd-Li^+ complex are of the T-type conformer with different orientations of the catecholic OHs.

As mentioned in the previous section, the T conformer is barely (~2 kJ mol^{-1}) more stable than the G1 conformer in the NAd-Li^+ complex. However, such a small energy difference cannot explain why only the T conformers are observed in the NAd-Li^+ complex. Factors such as the used level of theory and basis set as well as the fact that the zero-point energy corrections are included just at the harmonic level can certainly affect this energy difference. The conformational distribution for the NAd-Li^+ complex, together with the one for the NAd-Na^+ complex, will be discussed in Section III.e below.

d. Structural assignments of the NAd-Na^+ complex

Figures 9a-d show the IR dip spectra of the four conformers of the NAd-Na^+ complex

measured by examining the same bands probed to measure the UV-UV HB spectra. Differently from the NAd-Li^+ complex, the observed four IR dip spectra can be grouped into conformers A (Na) – B (Na) and C (Na) – D (Na) based on the following spectral features: (*i*) the free OH stretch of the amine chain is observed at 3,680 cm^{-1} in the former group while at 3,630 cm^{-1} in the latter, and (*ii*) the antisymmetric stretch of NH_2 is observed at 3,390 cm^{-1} in the former group while at 3,370 cm^{-1} in the latter. These results clearly support the presence of two different conformations of the amine chain. In addition, it is expected that the two conformers in each group have different orientations of the catecholic OHs. Since the IR spectra of conformers C (Na) and D (Na) are quite similar to those of the NAd-Li^+ complex, they can be assigned to T-type conformers. On the other hand, the IR spectra of conformers A (Na) and B (Na) are quite different from those of either the T- or the G1-type conformers of NAd-H^+ (see Figures 8e and 8f). Therefore, the input from quantum chemical calculations is necessary in order to assign their structures.

The computational protocol was the same with the one for the NAd-Li^+ complex. The calculated IR spectra of the stable 12 conformers presented in Figure 4 are shown in Figure 9e and the frequencies are presented in Table 4. In this complex, the intra-molecular frequencies of the H-bonded OH stretch of catechol are predicted to be at ~3,590 cm^{-1} for the T- and G1-type conformers, while those of the G2-type conformers are predicted to be ~10 cm^{-1} lower. The free OH stretch of the amine chain is predicted at higher frequency than that of catechol in the G1- and G2-type conformers except for G1-STR2, and at lower frequency in the T-type conformers. The spectral pattern of the latter coincides with that of conformers C (Na) and D (Na). Since it is difficult to determine which rotamers of the catecholic OHs are observed from their IR spectra alone, the assignment of conformers C (Na) and D (Na) to the T-STR1 and T-STR3 structures, respectively, was achieved by additionally taking into account their high stability from other rotamers (see Table 1). Comparing the spectra of conformers G1 and G2, significant differences appear in the free OH stretches. The free catecholic OH stretch is predicted at ~ 3,650 cm^{-1} in the G1-type conformers, while at 3,643 cm^{-1} in the G2-type conformers. In addition, the free OH stretches of the amine chain in the G1-type conformers are in the 3,649 – 3,680 cm^{-1} range, depending on the orientation of catecholic OHs, while almost at the constant value of 3,656 cm^{-1} in the G2-type conformers.

Such spectral features of the G2-type conformers do not match the experimental results, and thus they can be ruled out from the list of candidates for the conformers A (Na) and B (Na). By considering the frequency of the free OH stretch of the amine chain, conformer A (Na) is assigned to G1-STR1 or to G1-STR4, while conformer B (Na) to G1-STR3. These assignments are consistent with the spectral patterns in the NH stretching region: the frequencies of the antisymmetric stretch of the G1-type conformers (~3,380 cm^{-1} , except for STR, are 17 cm^{-1} higher than those of the T-type conformers at 3,363 cm^{-1}, in agreement with their difference of 20 cm^{-1} in the observed spectra.

The structural assignments can be further supported by considering the spectral features of the UV spectra. The conformer A (Na) exhibits a large red-shift. As reported in our previous paper,[12] similar red-shifts observed for NAd-H^+ were attributed to the $\pi\pi^*$-$\pi\sigma^*$ interaction in some folded structures, such as in the G1-type conformers. In addition, the strength of this interaction depends on the orientation of the catecholic OHs: conformers STR1 and STR2 are expected to exhibit such large red-shifts within the group of G1 conformers. Therefore, conformer A (Na) is assigned to G1-STR1.

e. Conformational distribution and specificity of NAd-Li^+ complex

For the NAd-Na^+ complex, two T-type conformers and two G1-type conformers (STR1 and STR3) have been identified as the observed ones. Within the G1-type conformers, STR1 and STR3 are ~6 kJ mol^{-1} more stable than other OH rotamers. Thus, the assignments of the G1-type conformers are appropriate. However, although the other two OH rotamers of the G1-type conformers are more stable than all the T-type conformers, two T-type conformers are observed instead of the G1-type conformers (STR2 and STR4). Such an inconsistency can be addressed by considering the relative free energies at room temperature, listed in Table 5. In ddition, in the NAd-Li^+ complex, although the observed two T-type conformers are less stable than the two G1-type conformers, only the T-type conformers are observed. Therefore, the conformational distribution cannot be explained by thermal equilibrium based on the relative isomer stability in the gas phase.

Similar inconsistencies were also previously observed for NAd-H^+, in which case

they were explained by kinetic trapping, i.e. the conformational distribution in solution remains through the desolvation process during the electrospray because of the high barrier to the more stable conformer in gas phase.[12] From this point of view, the conformer distribution observed in this work strongly reflects the one existing in solution. Therefore, the experimental finding that only the T-type conformers are observed in the NAd-Li^+ complex, while the G1-type conformers coexist in the NAd-H^+ and NAd-Na^+ complexes, supports the high stability of the T-type conformers of the NAd-Li^+ complex especially in solution. In other words, the NAd-Li^+ complex specifically prefers extended structural forms and as such it is quite different than the NAd-Na^+ complex.

IV. Conclusions

Conformer-selected UV and IR spectra of the NAd-Li^+ and NAd-Na^+ complexes produced by the electrospray ionization technique were measured under ultra-cold isolated conditions in a cold ion trap. In each complex, four different conformers were identified. Comparing the observed IR spectra with those of NAd-H^+, reported in our earlier study, and with the aid of quantum chemical calculations the structure of each conformer was assigned. Four conformers of NAd-Li^+ were assigned all having the T-type conformation on the amine chain but four different orientations of the catecholic OH groups. On the other hand, two conformers of NAd-Na^+ were assigned to G1-STR1 and G1-STR3 conformers and two others were to T-type conformers, which are similar to the case of NAd-H^+. The 8 observed conformers (4 for NAd-Li^+ and 4 for NAd-Na^+, which are a subset of the 12 + 12 optimized structures shown in Figures 3 and 4) are depicted in Figure 10.

The experimental finding that NAd-Li^+ favors the T conformer was reproduced by calculating relative stabilization energies. However, the T conformer is barely (~2 kJ mol^{-1}) more stable than the G1 conformer and such a small energy difference cannot explain why NAd-Li^+ forms only the T-type conformers in the gas phase. This finding suggests that the complexes may still retain their solution conformer distribution by kinetic trapping through the electrospray process. The experimental finding that only the T conformers are observed in NAd-Li^+ complex demonstrates that it is highly stable in solution. In other words, NAd-

Li^+ specifically prefers such an extended structure in solution, which is quite different from the ones preferred by both NAd-Na^+ and NAd-H^+. This structural specificity of the NAd-Li^+ complex can explain why the Li^+ cation affects, via its conformational modulation, several molecular recognition processes concerning NAd.

Acknowledgments: This work was supported in part by KAKENHI (JP205104008) on innovative area (2503), KAKENHI (JP15H02157, JP15K13620, JP16H06028) of JSPS, the World Research Hub Initiative (WRHI) of Tokyo Institute of Technology, and the Cooperative Research Program of the "Network Joint Research Center for Materials and Devices" from the Ministry of Education, Culture, Sports, Science and Technology (MEXT), Japan. SSX acknowledges support from the U.S. Department of Energy, Office of Science, Office of Basic Energy Sciences, Division of Chemical Sciences, Geosciences and Biosciences at Pacific Northwest National Laboratory. Battelle operates the Pacific Northwest National Laboratory for the U.S. Department of Energy.

Table 1. Relative stabilization energies of the various stable conformers of the NAd-Li^+ and NAd-Na^+ complexes.

Conformer	Relative stabilization energy with ZPE / kJ mol^{-1}	
	Li^+ complex	Na^+ complex
T-STR1	0	7.11
T-STR2	6.96	14.18
T-STR3	2.03	9.22
T-STR4	5.36	12.42
G1-STR1	2.22	0.60
G1-STR2	15.1	5.84
G1-STR3	3.52	0
G1-STR4	7.84	6.20
G2-STR1	9.53	12.0
G2-STR2	9.68	11.6
G2-STR3	8.27	12.2
G2-STR4	11.0	14.5

Table 2. 0-0 transition energies of the NAd-Li^+ and NAd-Na^+ complexes.

Conformer	0-0 transition energy / cm^{-1}
A (Li)	34,962
B (Li)	34,973
C (Li)	35,150
D (Li)	35,165
A (Na)	34,038
B (Na)	34,978
C (Na)	35,037
D (Na)	35,147

Table 3. Observed (A – D) and calculated frequencies of the N-H and O-H stretches of the various conformers of the NAd-Li^+ complex.

Conformer	NH stretches		OH stretches		
	Sym	Anti	catechol H-bonded	amine chain	catechol free
A (obs.)	3321	3374	3594	3640	3657
B (obs.)	3320	3375	3594	3541	3657
C (obs.)	3318	3373	3595	3638	3658
D (obs.)	3314	3378	3593	3638	3658
T-1	3285	3365	3596	3647	3654
T-2	3287	3365	3595	3644	3663
T-3	3287	3366	3595	3647	3657
T-4	3287	3365	3592	3644	3662
G1-1	3275	3367	3591	3656	3655
G1-2	3272	3364	3600	3661	3667
G1-3	3277	3368	3592	3661	3658
G1-4	3273	3366	3594	3653	3658
G2-1	3273	3354	3580	3666	3644
G2-2	3274	3354	3585	3675	3641
G2-3	3274	3355	3580	3668	3642
G2-4	3273	3354	3584	3664	3643

Table 4. Observed (A – D) and calculated frequencies of the N-H and O-H stretches of the various conformers of the NAd-Na^+ complex.

Conformer	NH stretches		OH stretches		
	Sym	Anti	catechol H-bonded	amine chain	catechol free
A (obs.)	—	3390	3587	3683	3656
B (obs.)	—	3391	3587	3677	3656
C (obs.)	—	3371	3594	3633	3658
D (obs.)	—	3371	3593	3631	3659
T-1	3285	3363	3597	3637	3657
T-2	3284	3363	3598	3635	3666
T-3	3285	3363	3597	3638	3660
T-4	3284	3363	3595	3634	3664
G1-1	3291	3377	3585	3680	3652
G1-2	3311	3392	3589	3649	3650
G1-3	3299	3383	3587	3659	3649
G1-4	3293	3379	3592	3678	3651
G2-1	3280	3358	3582	3656	3643
G2-2	3279	3356	3584	3656	3641
G2-3	3280	3357	3582	3657	3644
G2-4	3279	3356	3583	3656	3645

Table 5. Relative Gibbs free energies (at 300 K) of the various stable conformers of the NAd-Li^+ and NAd-Na^+ complexes.

Conformer	Relative Gibbs free energy / kJ mol^{-1}	
	Li^+ complex	Na^+ complex
T-STR1	0	4.13
T-STR2	6.68	10.8
T-STR3	1.58	5.68
T-STR4	4.98	9.03
G1-STR1	2.13	0.78
G1-STR2	14.1	6.23
G1-STR3	7.31	0
G1-STR4	7.53	6.57
G2-STR1	12.5	12.0
G2-STR2	12.4	12.0
G2-STR3	11.3	12.1
G2-STR4	14.2	14.5

Figure 1. The three types of stable conformations of NAd-H^+. Additional rotamers of the catecholic OHs exist for each type of conformation.

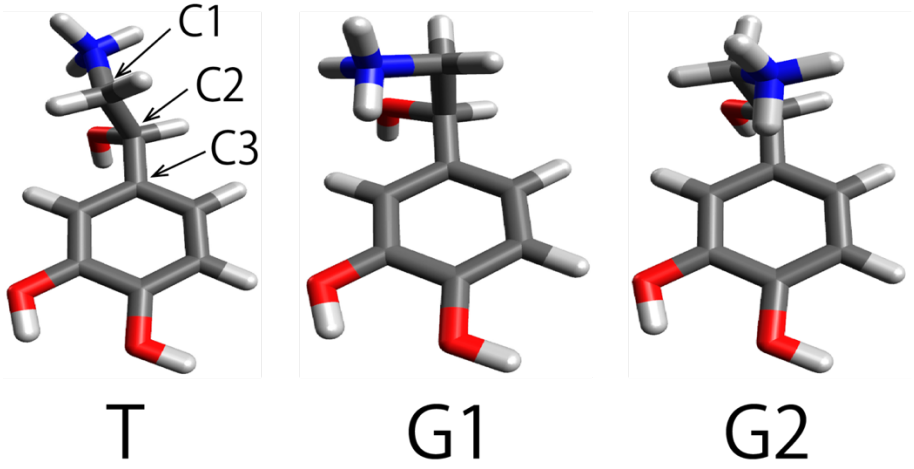

Figure 2. Calculated 2-dimensional potential energy surface of a) NAd-Li^+ and b) NAd-Na^+.

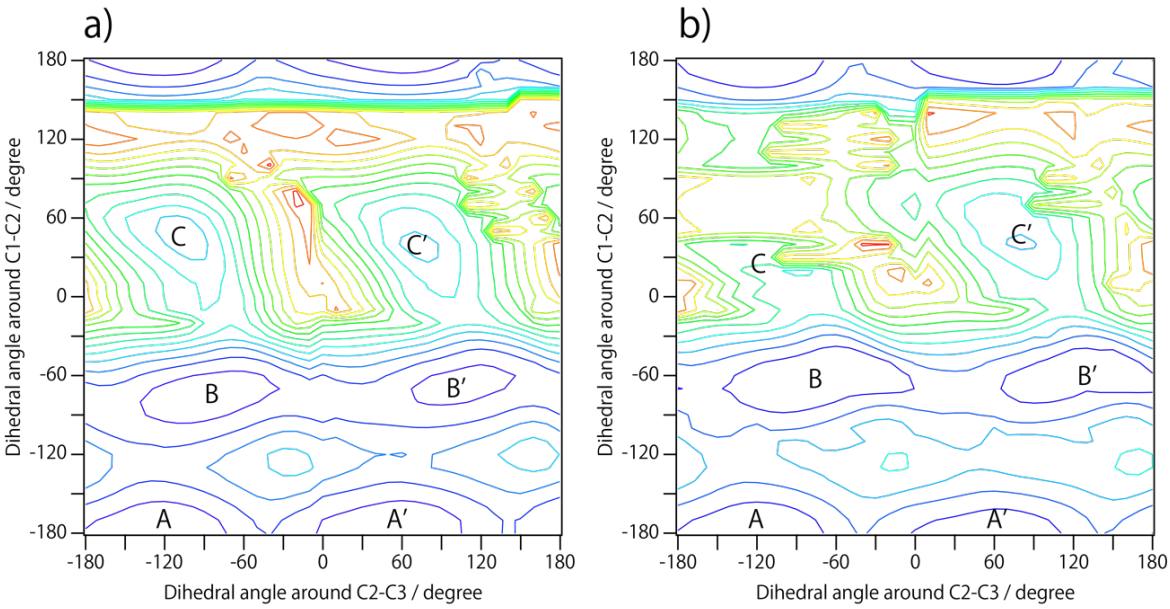

Figure 3. Optimized structures of the NAd-Li^+ complex calculated at the RI-CC2/aug-cc-pVDZ level of theory.

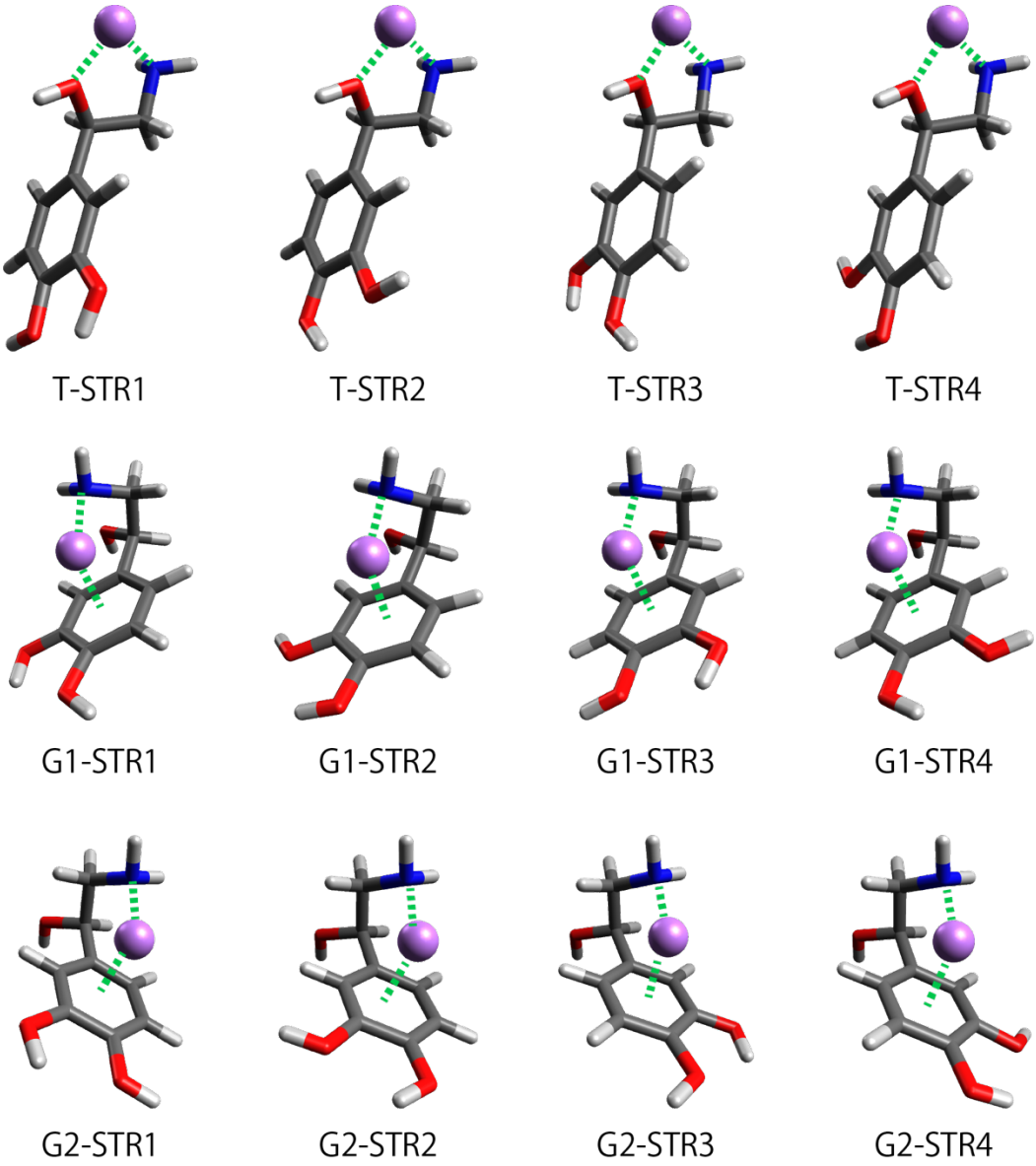

Figure 4. Optimized structures of the NAd-Na^+ complex calculated at the RI-CC2/aug-cc-pVDZ level of theory.

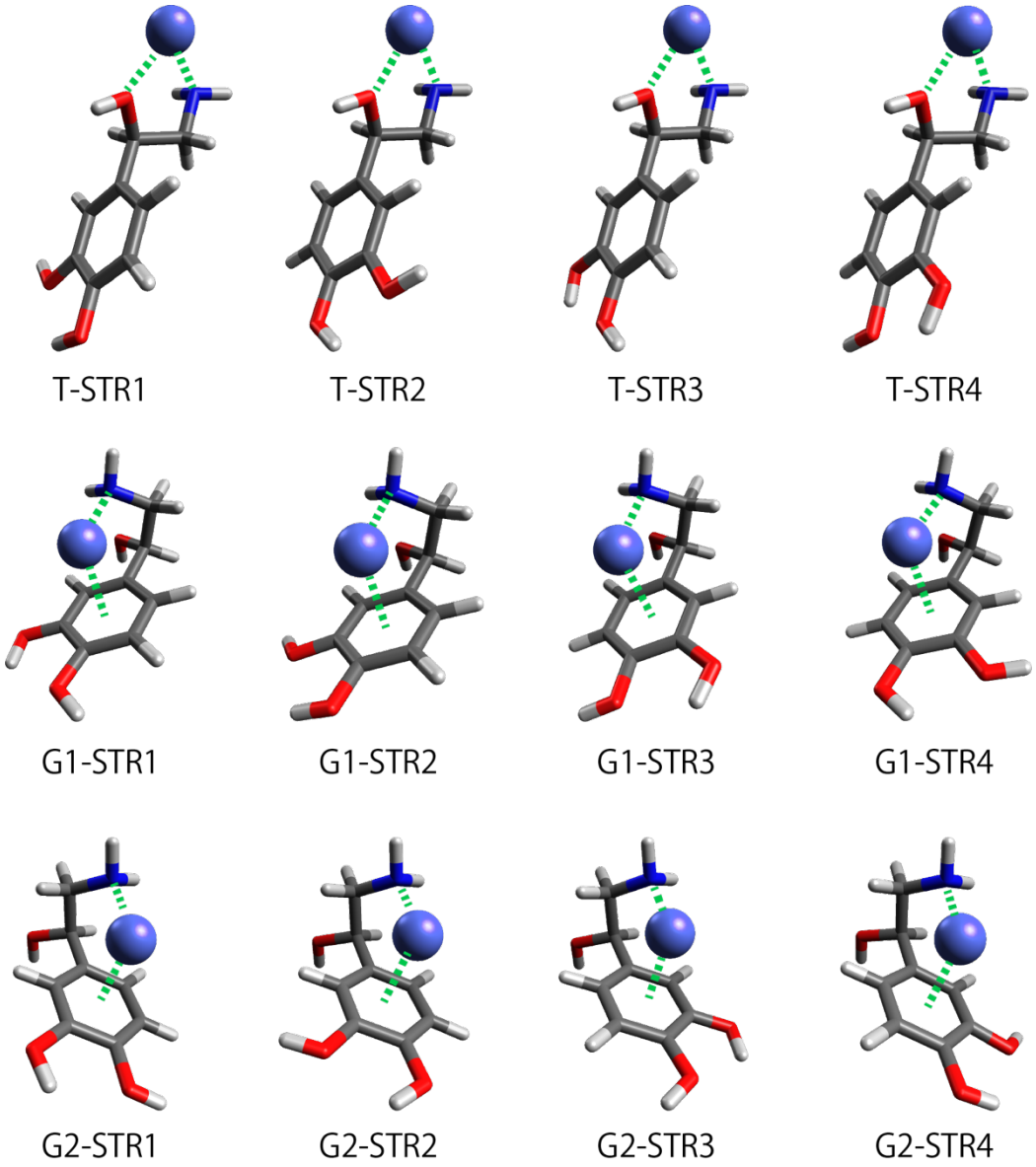

Figure 5. UVPD spectra of a) NAd-Li^+, b) NAd-Na^+ and c) NAd-H^+.

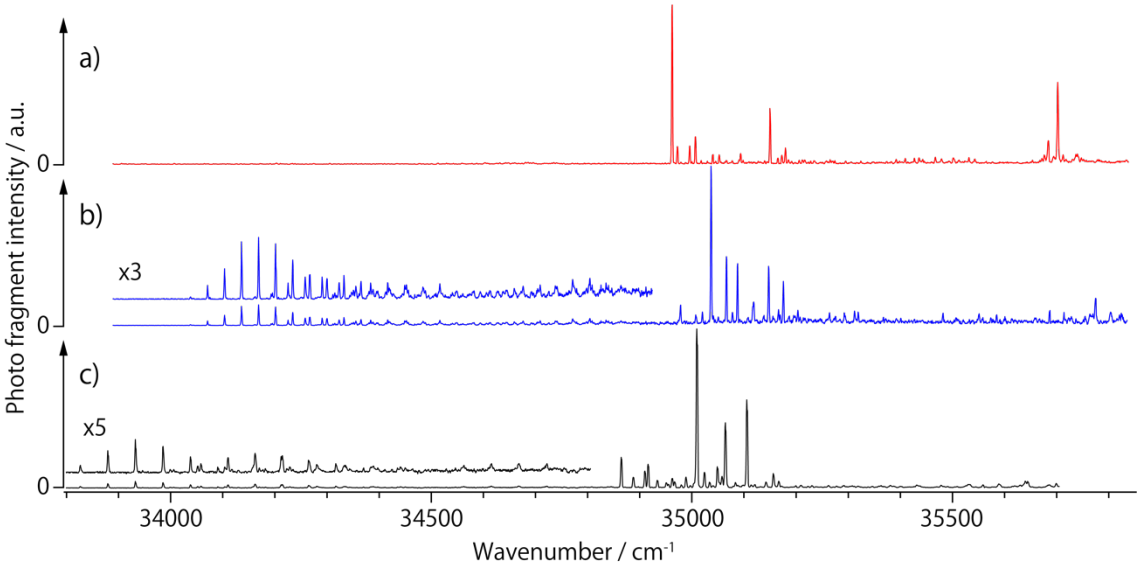

Figure 6. a) UV-UV HB and b) UVPD spectra of NAd-Li^+. The UV-UV HB spectra A-D were respectively measured by probing bands A-D observed in the UVPD spectrum.

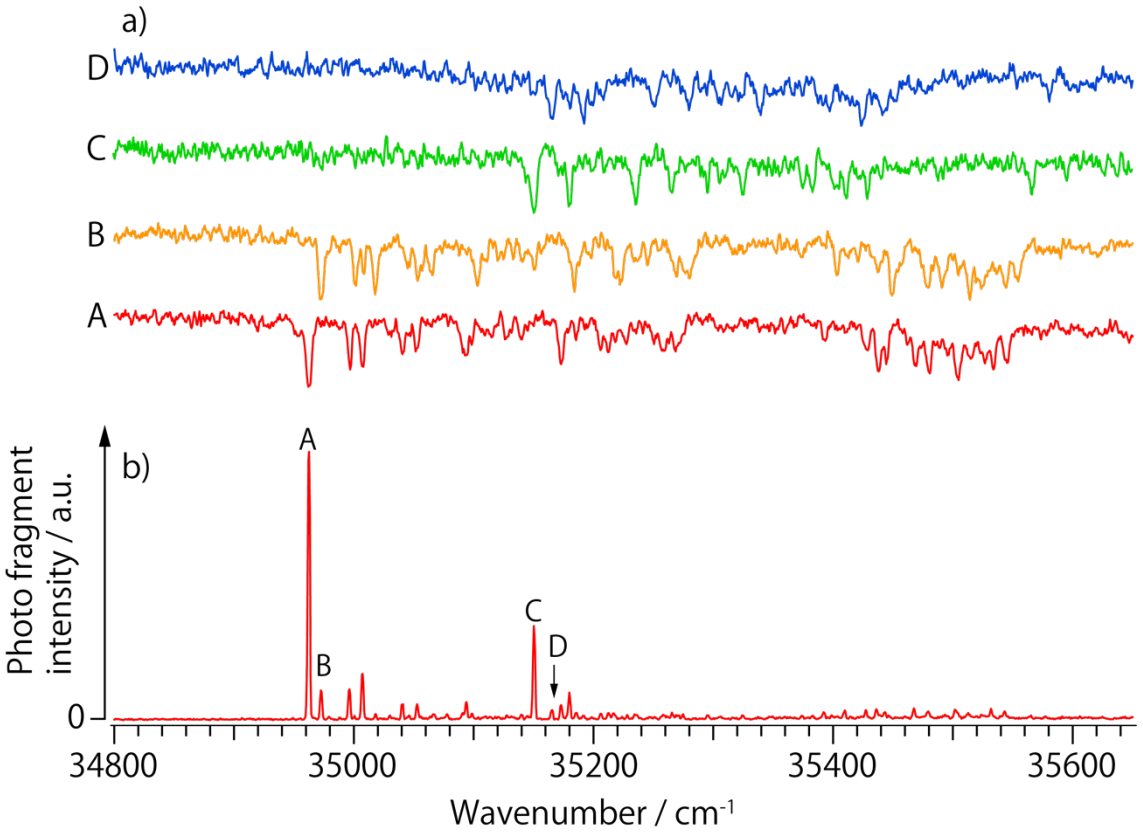

Figure 7. a) UV-UV HB and b) UVPD spectra of NAd-Na^+. The UV-UV HB spectra A-D were respectively measured by probing bands A-D observed in the UVPD spectrum.

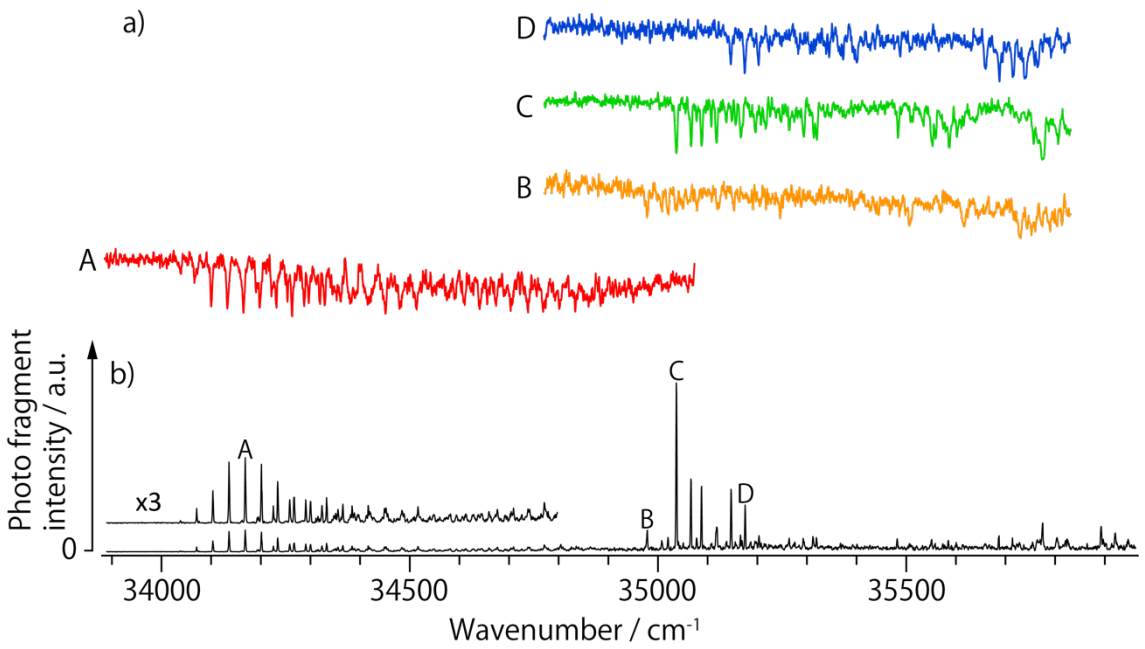

Figure 8. IR dip spectra of a-d) NAd-Li^+, e) T and f) G1 conformers of NAd-H^+, and g) calculated IR spectra of NAd-Li^+. The intensity of NH stretching region in the calculated spectra is expanded fivefold.

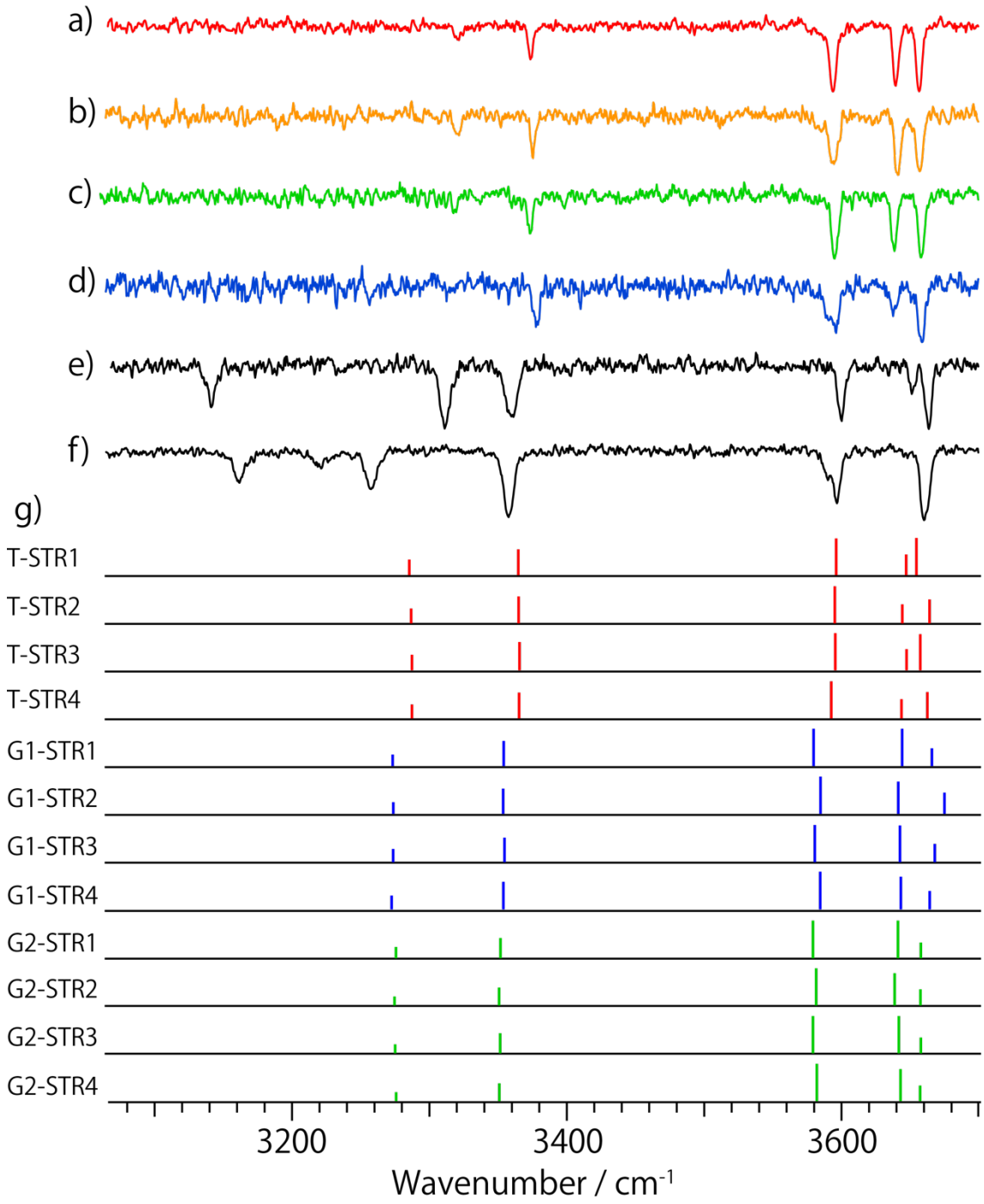

Figure 9. IR dip spectra of a-d) NAd-Na^+, e) T and f) G1 conformers of NAd-H^+, and g) calculated IR spectra of NAd-Na^+. The NH stretching region was also measured by increasing the IR laser energy. The intensity of that region in the calculated spectra is expanded fivefold.

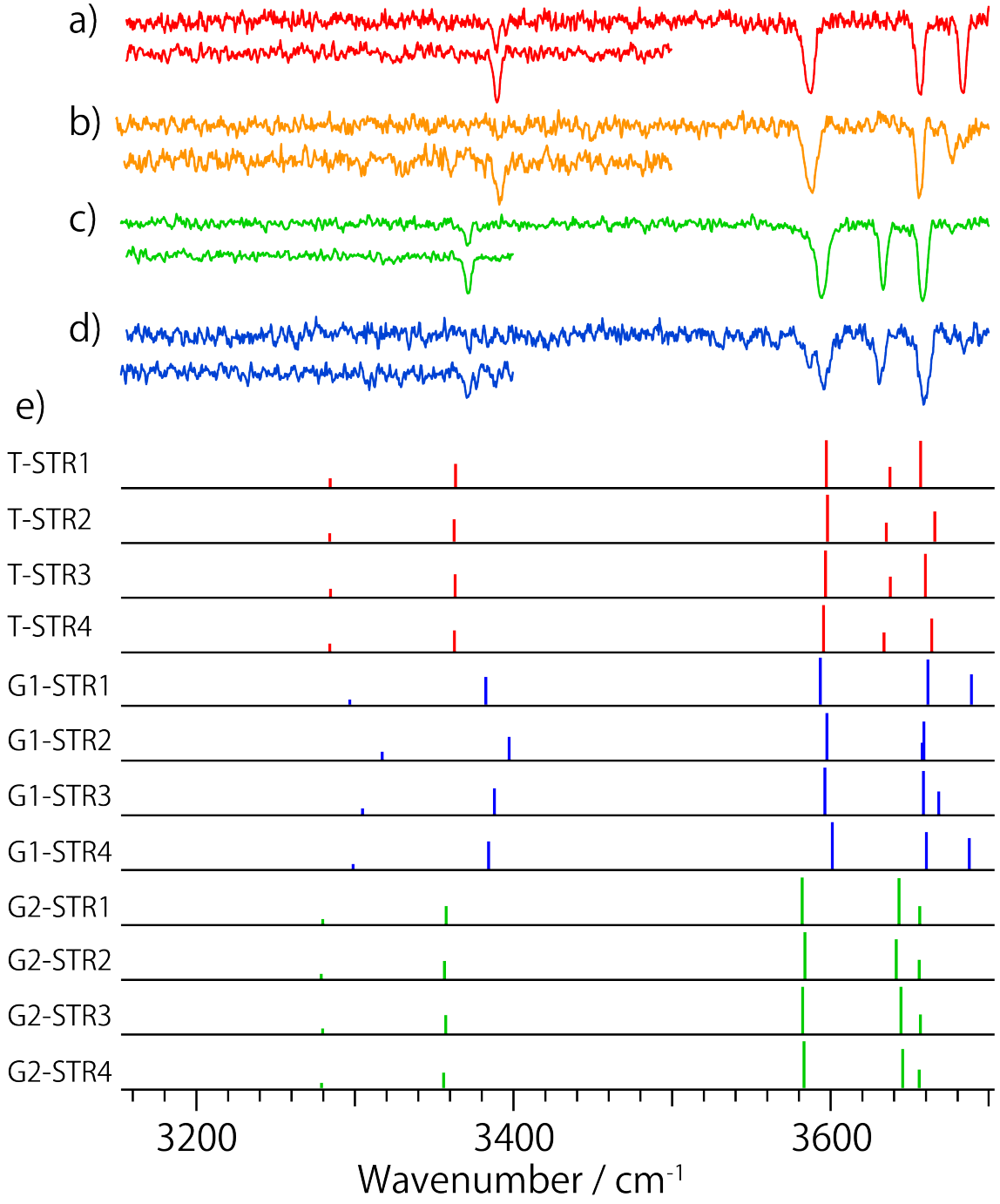

Figure 10. Observed conformers for the NAd-Li^+ and NAd-Na^+ complexes.

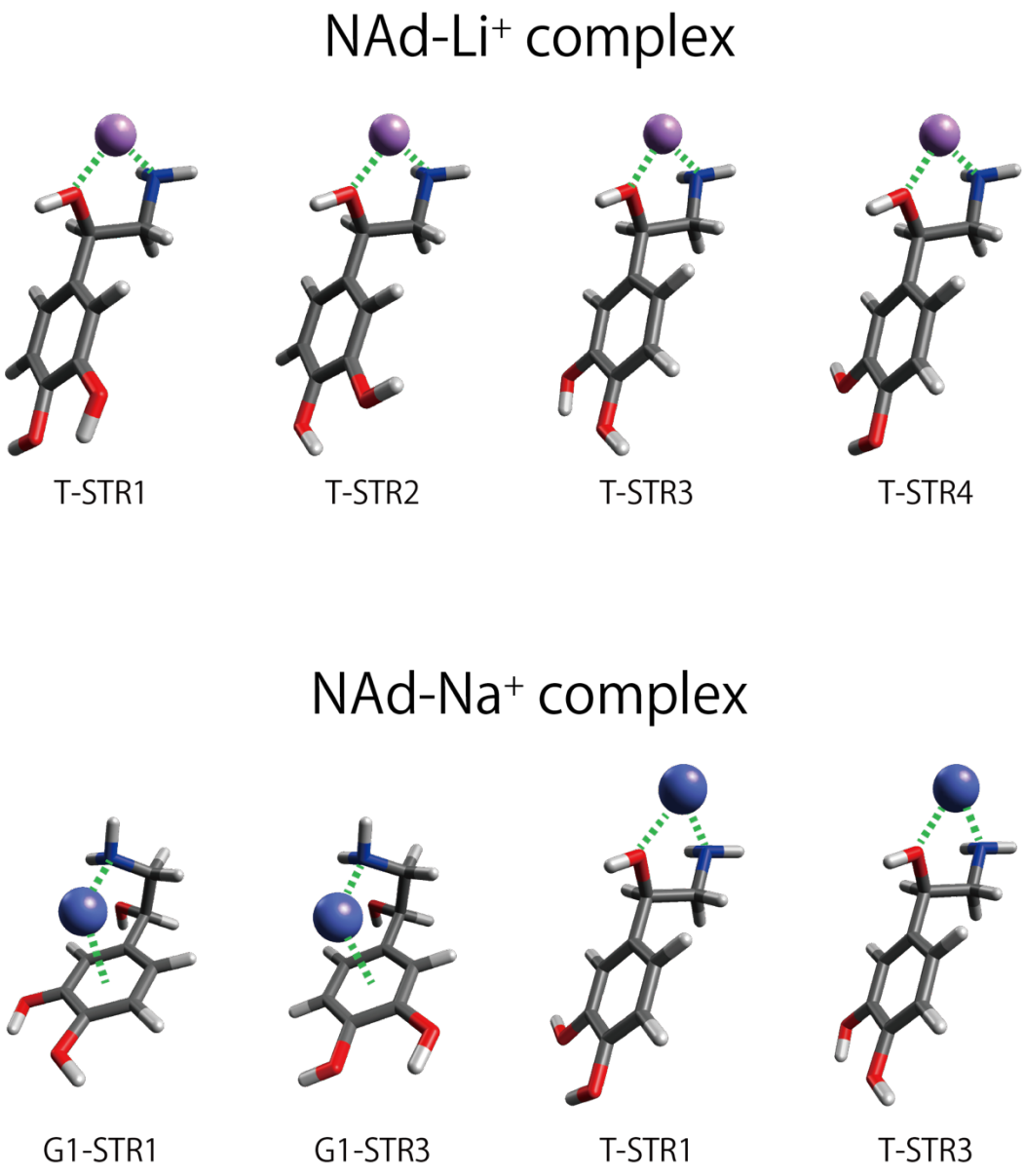

References

1. Can, A.; Schulze, T. G.; Gould, T. D. *Pharmacol. Biochem. Behav.* **2014,** *123*, 3-16.
2. Cade, J. F. J. *Med. J. Aust.* **1949,** *2*, 349-352.
3. Ohnishi, T.; Murata, T.; Watanabe, A.; Hida, A.; Ohba, H.; Iwayama, Y.; Mishima, K.; Gondo, Y.; Yoshikawa, T. *J. Biol. Chem.* **2014,** *289*, 10785-96.
4. Marmol, F. *Prog. Neuro-Psychopharmacol. Biol. Psychiatry* **2008,** *32*, 1761-1771.
5. Shaldubina, A.; Agam, G.; Belmaker, R. H. *Prog. Neuro-Psychopharmacol. Biol. Psychiatry* **2001,** *25*, 855-866.
6. Berridge, M. J.; Downes, C. P.; Hanley, M. R. *Cell* **1989,** *59*, 411-419.
7. Lack, B.; Daya, S.; Nyokong, T. *J. Pineal Res.* **2001,** *31*, 102-108.
8. Walid, O. S.; Esther, S.; Robert, G.; Ellen, H.; Javaid, J.; David, B. B. *Journal of Child Neurology* **1987,** *2*, 50-56.
9. Biederman, J.; Spencer, T. *Biol Psychiat* **1999,** *46*, 1234-1242.
10. Biederman, J. *Biol Psychiat* **2005,** *57*, 1215-1220.
11. Nagy, P. I.; Alagona, G.; Ghio, C.; Takács-Novák, K. *J. Am. Chem. Soc.* **2003,** *125*, 2770-2785.
12. Wako, H.; Ishiuchi, S.-i.; Kato, D.; Feraud, G.; Dedonder-Lardeux, C.; Jouvet, C.; Fujii, M. *Phys. Chem. Chem. Phys.* **2017,** *19*, 10777-10785.
13. Snoek, L. C.; Van Mourik, T.; Simons, J. P. *Mol. Phys.* **2003,** *101*, 1239-1248.
14. Snoek, L. C.; Van Mourik, T.; Çarçabal, P.; Simons, J. P. *Phys. Chem. Chem. Phys.* **2003,** *5*, 4519-4526.
15. Macleod, N. A.; Robertson, E. G.; Simons, J. P. *Mol. Phys.* **2003,** *101*, 2199-2210.
16. Graham, R. J.; Kroemer, R. T.; Mons, M.; Robertson, E. G.; Snoek, L. C.; Simons, J. P. *J. Phys. Chem. A* **1999,** *103*, 9706-9711.
17. Park, M.-K.; Yoo, H.-S.; Kang, Y. K.; Lee, N.-S. *B Korean Chem Soc* **1992,** *13*, 230 - 235.
18. Šolmajer, P.; Kocjan, D.; Šolmajer, T., Conformational Study of Catecholamines in Solution. In *Zeitschrift für Naturforschung C*, 1983; Vol. 38, p 758.
19. Scherzer, W.; Krätzschmar, O.; Selzle, H. L.; Schlag, E. *Z. Naturforsch.* **1992,** *47a*, 1248-1252.
20. Page, R. H.; Shen, Y. R.; Lee, Y. T. *J. Chem. Phys.* **1988,** *88*, 5362-5376.

21. Wolk, A. B.; Leavitt, C. M.; Garand, E.; Johnson, M. A. *Acc. Chem. Res.* **2014,** *47*, 202-210.
22. Leavitt, C. M.; Wolk, A. B.; Fournier, J. A.; Kamrath, M. Z.; Garand, E.; Van Stipdonk, M. J.; Johnson, M. A. *J. Phys. Chem. Lett.* **2012,** *3*, 1099-1105.
23. Garand, E.; Kamrath, M. Z.; Jordan, P. A.; Wolk, A. B.; Leavitt, C. M.; McCoy, A. B.; Miller, S. J.; Johnson, M. A. *Science* **2012,** *335*, 694-8.
24. Kamrath, M. Z.; Relph, R. A.; Guasco, T. L.; Leavitt, C. M.; Johnson, M. A. *Int. J. Mass Spectrom.* **2011,** *300*, 91-98.
25. Kamrath, M. Z.; Garand, E.; Jordan, P. A.; Leavitt, C. M.; Wolk, A. B.; Van Stipdonk, M. J.; Miller, S. J.; Johnson, M. A. *J. Am. Chem. Soc.* **2011,** *133*, 6440-8.
26. Chin, W.; Piuzzi, F.; Dimicoli, I.; Mons, M. *Phys. Chem. Chem. Phys.* **2006,** *8*, 1033-1048.
27. Dean, J. C.; Burke, N. L.; Hopkins, J. R.; Redwine, J. G.; Ramachandran, P. V.; McLuckey, S. A.; Zwier, T. S. *The journal of physical chemistry. A* **2015,** *119*, 1917-32.
28. Buchanan, E. G.; James, W. H., 3rd; Choi, S. H.; Guo, L.; Gellman, S. H.; Muller, C. W.; Zwier, T. S. *J. Chem. Phys.* **2012,** *137*, 094301.
29. James, W. H., 3rd; Baquero, E. E.; Choi, S. H.; Gellman, S. H.; Zwier, T. S. *J. Phys. Chem. A* **2010,** *114*, 1581-91.
30. Ishiuchi, S.; Wako, H.; Kato, D.; Fujii, M. *J. Mol. Spectrosc.* **2017,** *332*, 45-51.
31. Sohn, W. Y.; Ishiuchi, S.; Çarçabal, P.; Oba, H.; Fujii, M. *Chem. Phys.* **2014,** *445*, 21-30.
32. Sohn, W. Y.; Ishiuchi, S.; Miyazaki, M.; Kang, J.; Lee, S.; Min, A.; Choi, M. Y.; Kang, H.; Fujii, M. *Phys. Chem. Chem. Phys.* **2013,** *15*, 957-964.
33. Shimozono, Y.; Yamada, K.; Ishiuchi, S.; Tsukiyama, K.; Fujii, M. *Phys. Chem. Chem. Phys.* **2013,** *15*, 5163-5175.
34. Ishiuchi, S.; Mitsuda, H.; Asakawa, T.; Miyazaki, M.; Fujii, M. *Phys. Chem. Chem. Phys.* **2011,** *13*, 7812-7820.
35. Ishiuchi, S.; Asakawa, T.; Mitsuda, H.; Miyazaki, M.; Chakraborty, S.; Fujii, M. *J. Phys. Chem. A* **2011,** *115*, 10363-10369.
36. Mitsuda, H.; Miyazaki, M.; Nielsen, I. B.; Çarçabal, P.; Dedonder, C.; Jouvet, C.; Ishiuchi, S.; Fujii, M. *J. Phys. Chem. Lett.* **2010,** *1*, 1130-1133.

37. Stearns, J. A.; Seaiby, C.; Boyarkin, O. V.; Rizzo, T. R. *Phys. Chem. Chem. Phys.* **2009,** *11*, 125-32.
38. Stearns, J. A.; Guidi, M.; Boyarkin, O. V.; Rizzo, T. R. *J. Chem. Phys.* **2007,** *127*, 154322.
39. Stearns, J. A.; Boyarkin, O. V.; Rizzo, T. R. *J. Am. Chem. Soc.* **2007,** *129*, 13820-1.
40. Kamariotis, A.; Boyarkin, O. V.; Mercier, S. R.; Beck, R. D.; Bush, M. F.; Williams, E. R.; Rizzo, T. R. *J. Am. Chem. Soc.* **2006,** *128*, 905-16.
41. Rodrigo, C. P.; James, W. H., 3rd; Zwier, T. S. *J. Am. Ceram. Soc.* **2011,** *133*, 2632-41.
42. Buchanan, E. G.; James, W. H., 3rd; Gutberlet, A.; Dean, J. C.; Guo, L.; Gellman, S. H.; Zwier, T. S. *Faraday Discuss.* **2011,** *150*, 209-26; discussion 257-92.
43. Zwier, T. S. *Nat. Chem.* **2009,** *1*, 687-8.
44. Marsh, B. M.; Voss, J. M.; Garand, E. *J. Chem. Phys.* **2015,** *143*, 204201.
45. Nagornova, N. S.; Rizzo, T. R.; Boyarkin, O. V. *Science* **2012,** *336*, 320-3.
46. Wolke, C. T.; Fournier, J. A.; Miliordos, E.; Kathmann, S. M.; Xantheas, S. S.; Johnson, M. A. *J. Chem. Phys.* **2016,** *144*, 074305.
47. Miliordos, E.; Aprà, E.; Xantheas, S. S. *J Chem Theory Comput* **2016,** *12*, 4004-4014.
48. Fournier, J. A.; Wolke, C. T.; Johnson, M. A.; Odbadrakh, T. T.; Jordan, K. D.; Kathmann, S. M.; Xantheas, S. S. *J. Phys. Chem. A* **2015,** *119*, 9425-9440.
49. Johnson, C. J.; Dzugan, L. C.; Wolk, A. B.; Leavitt, C. M.; Fournier, J. A.; McCoy, A. B.; Johnson, M. A. *J. Phys. Chem. A* **2014,** *118*, 7590-7597.
50. McCoy, A. B. *J. Phys. Chem. B* **2014,** *118*, 8286-8294.
51. Breen, K. J.; DeBlase, A. F.; Guasco, T. L.; Voora, V. K.; Jordan, K. D.; Nagata, T.; Johnson, M. A. *J. Phys. Chem. A* **2012,** *116*, 903-912.
52. Deible, M. J.; Tuguldur, O.; Jordan, K. D. *J. Phys. Chem. B* **2014,** *118*, 8257-8263.
53. Galimberti, D. R.; Milani, A.; Tommasini, M.; Castiglioni, C.; Gaigeot, M.-P. *J Chem Theory Comput* **2017,** *13*, 3802-3813.
54. Bakker, D. J.; Dey, A.; Tabor, D. P.; Ong, Q.; Mahe, J.; Gaigeot, M. P.; Sibert, E. L.; Rijs, A. M. *Phys. Chem. Chem. Phys.* **2017,** *19*, 20343-20356.
55. Fagiani, M. R.; Knorke, H.; Esser, T. K.; Heine, N.; Wolke, C. T.; Gewinner, S.; Schollkopf, W.; Gaigeot, M. P.; Spezia, R.; Johnson, M. A.; Asmis, K. R. *Phys. Chem. Chem. Phys.* **2016,** *18*, 26743-26754.

56. Svendsen, A.; Lorenz, U. J.; Boyarkin, O. V.; Rizzo, T. R. *Rev. Sci. Instrum.* **2010,** *81*, 073107.
57. Boyarkin, O. V.; Mercier, S. R.; Kamariotis, A.; Rizzo, T. R. *J. Am. Chem. Soc.* **2006,** *128*, 2816-7.
58. Kang, H.; Féraud, G.; Dedonder-Lardeux, C.; Jouvet, C. *J. Phys. Chem. Lett.* **2014,** *5*, 2760-2764.
59. Okuzawa, Y.; Fujii, M.; Ito, M. *Chem. Phys. Lett.* **1990,** *171*, 341-346.
60. Frisch, M. J.; Trucks, G. W.; Schlegel, H. B.; Scuseria, G. E.; Robb, M. A.; Cheeseman, J. R.; Scalmani, G.; Barone, V.; Mennucci, B.; Petersson, G. A.; Nakatsuji, H.; Caricato, M.; Li, X.; Hratchian, H. P.; Izmaylov, A. F.; Bloino, J.; Zheng, G.; Sonnenberg, J. L.; Hada, M.; Ehara, M.; Toyota, K.; Fukuda, R.; Hasegawa, J.; Ishida, M.; Nakajima, T.; Honda, Y.; Kitao, O.; Nakai, H.; Vreven, T.; Montgomery, J. A.; Peralta, J. E.; Ogliaro, F.; Bearpark, M.; Heyd, J. J.; Brothers, E.; Kudin, K. N.; Staroverov, V. N.; Kobayashi, R.; Normand, J.; Raghavachari, K.; Rendell, A.; Burant, J. C.; Iyengar, S. S.; Tomasi, J.; Cossi, M.; Rega, N.; Millam, J. M.; Klene, M.; Knox, J. E.; Cross, J. B.; Bakken, V.; Adamo, C.; Jaramillo, J.; Gomperts, R.; Stratmann, R. E.; Yazyev, O.; Austin, A. J.; Cammi, R.; Pomelli, C.; Ochterski, J. W.; Martin, R. L.; Morokuma, K.; Zakrzewski, V. G.; Voth, G. A.; Salvador, P.; Dannenberg, J. J.; Dapprich, S.; Daniels, A. D.; Farkas; Foresman, J. B.; Ortiz, J. V.; Cioslowski, J.; Fox, D. J. *Gaussian 09, Revision B.01*, Wallingford CT, 2009.
61. Ahlrichs, R.; Bär, M.; Häser, M.; Horn, H.; Kölmel, C. *Chem. Phys. Lett.* **1989,** *162*, 165-169.

TOC

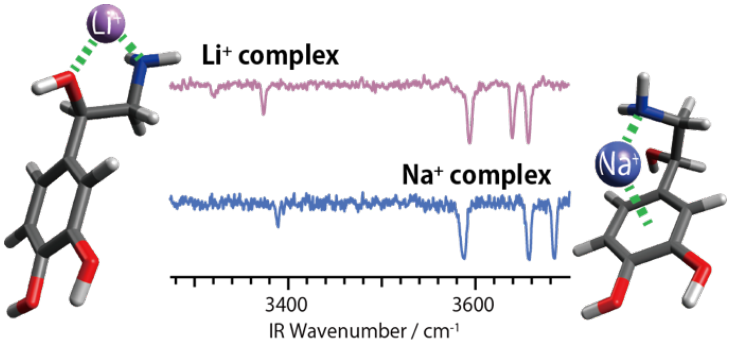

Noradrenaline favors an extended conformation when coordinating to Li^+ when compared to Na^+, which may explain the the tranquilizing effect of Li^+.